Hemilabile P–Alkene Ligands in Chiral Rhodium and Copper Complexes: Catalytic Asymmetric 1,4 Additions to Enones. 2†,(1)

ARTICLE *in* ORGANOMETALLICS · APRIL 2010

Impact Factor: 4.13 · DOI: 10.1021/om100248u

4 AUTHORS, INCLUDING:

Alexander Briceño
Venezuelan Institute for Scientific Research
77 PUBLICATIONS **526** CITATIONS
SEE PROFILE

Romano Dorta
Simon Bolívar University
34 PUBLICATIONS **716** CITATIONS
SEE PROFILE

ORGANOMETALLICS
Article

Organometallics **2010,** *29,* 2503–2514 2503
DOI: 10.1021/om100248u

Hemilabile P-Alkene Ligands in Chiral Rhodium and Copper Complexes: Catalytic Asymmetric 1,4 Additions to Enones. 2[†,1]

Emma Drinkel,[‡] Alexander Briceño,[§] Reto Dorta,[‡] and Romano Dorta*[,∥]

[‡]*Organisch-Chemisches Institut (OCI), Universität Zürich, Winterthurerstrasse 190, CH-8057, Zurich, Switzerland,* [§]*Centro de Química, Instituto Venezolano de Investigaciones Científicas (IVIC), Altos de Pipe, Venezuela, and* [∥]*Departamento de Química, Universidad Simón Bolívar, Caracas 1080A, Venezuela*

Received March 30, 2010

Two equivalents of the chiral dibenz[*b*,*f*]azepine-derived P-alkene ligands **2**−**6** per metal afforded mononuclear Rh(I) and Cu(I) complexes that were used as catalysts for asymmetric conjugate addition reactions. Rh formed square-planar neutral (**8**−**10**) and cationic complexes (**11**, **12**) of the general formulas [RhCl(κ^1P-alkene)(κ^2P-alkene)] and *cis*-[Rh(κ^2P-alkene)$_2$][BF_4], respectively (P-alkene = **2**, **5**, **6**). In both cases reversible decoordination of the alkene function of the bidentate P-alkene ligands was observed in the presence of Lewis basic solvents, and model compounds of mono- and bis-solvated species (**13**, **14**) were isolated. Cu formed trigonal-planar neutral (**15**−**17**) and cationic complexes (**18**, **19**) of the general formulas [CuI(κ^1P-alkene)$_2$] and [Cu(κ^1P-alkene)$_2$$BF_4$], respectively (P-alkene = **2**, **4**, **5**). The cationic Rh species **11** catalyzed the 1,4-addition of arylboronic acids to cyclic and linear enones with high activities (TON = 62 at 40 °C) and excellent enantiocontrol (up to 99% ee) for a wide range of substrates. The cationic Cu complex **18** catalyzed the 1,4-addition of Al(C_2H_5)$_3$ to 2-cyclohexenone with 39% ee.

Introduction

Chiral alkene ligands[2] and, in particular, chiral P-alkene ligands[3] with improved stability are attracting growing interest in the field of enantioselective catalysis. Grützmacher et al. introduced the highly effective tropylidene and dibenz[*b*,*f*]azepine molecules as alkene-bearing entities in P-alkene and N-alkene ligand systems, respectively.[4] Chiral variants of tropylidene (ligand **1**) and dibenz[*b*,*f*]azepine derivatives (ligands **2**−**6**) are depicted in Chart 1. The chiral phosphine−alkene ligand **1** yielded optically enriched amines with up to 86% ee in Ir-catalyzed asymmetric imine hydrogenations.[5] We have recently developed a general and facile method for the preparation of dibenz[*b*,*f*]azepine-derived chiral P-alkene ligands, of which **2**−**6** are examples (note that ligands **4** and **6** possess stereogenic P atoms).[1] The alkene−phosphoramidite **2**[6] was used as a ligand in the Ir-catalyzed enantioselective formation of allylic amines from allylic alcohols (70% ee)[7] and for the Rh-catalyzed conjugate addition (CA) of arylboronic acids to enones with up to 92% ee.[1]

The enantioselective CA of carbon nucleophiles to enones is an important synthetic tool for the construction of stereogenic C−C bonds, and Rh- and Cu-based chiral complexes are among the most useful catalysts for this transformation. Rh-catalyzed enantioselective CA reactions with boronic acid nucleophiles were very successfully achieved, inter alia,[8] with chiral phosphoramidites[9] and chiral dienes,[10] each on their own, and combined as chiral bidentate

[†] In memory of Carlo Floriani.

*To whom correspondence should be addressed. Fax: +58 212 9063961. E-mail: rdorta@usb.ve.

(1) Part 1: Mariz, R.; Briceño, A.; Dorta, R.; Dorta, R. *Organometallics* **2008**, *27*, 6605.

(2) For a review, see: Defieber, C.; Grützmacher, H.; Carreira, E. *Angew. Chem., Int. Ed.* **2008**, *47*, 4482.

(3) (a) Shintani, R.; Duan, W.-L.; Nagano, T.; Okada, A.; Hayashi, T. *Angew. Chem., Int. Ed.* **2005**, *44*, 4611. (b) Duan, W.-L.; Iwamura, H.; Shintani, R.; Hayashi, T. *J. Am. Chem. Soc.* **2007**, *129*, 2130. (c) Shintani, R.; Duan, W.-L.; Okamoto, K.; Hayashi, T. *Tetrahedron: Asymmetry* **2005**, *16*, 3400. (d) Kasák, P.; Arion, V. B.; Widhalm, M. *Tetrahedron: Asymmetry* **2006**, *17*, 3084.

(4) (a) Schönberg, H.; Boulmaâz, S.; Wörle, M.; Liesum, L.; Schweiger, A.; Grützmacher, H. *Angew. Chem., Int. Ed.* **1998**, *37*, 1423. (b) Boulmaâz, S.; Mlakar, M.; Loss, S.; Schönberg, H.; Deblon, S.; Wörle, M.; Nesper, R.; Grützmacher, H. *Chem. Commun.* **1998**, 2623. (c) Büttner, T.; Breher, F.; Grütcher, H. *Chem. Commun.* **2004**, 2820. (d) Maire., P.; Büttner, T.; Breher, F.; LeFloch, P.; Grützmacher, H. *Angew. Chem., Int. Ed.* **2005**, *44*, 6318. (e) Büttner, T.; Geier, J.; Frison, G.; Harmer, J.; Calle, C.; Schweiger, A.; Schönberg, H.; Grützmacher, H. *Science* **2005**, *307*, 235. For additional examples of chiral tropylidene and achiral dibenzazepine derived ligands, see: Deblon, S; Grützmacher, H.; Maire, P.; Schönberg, H. WO 03/048175 A1.

(5) Maire, P.; Deblon, S.; Breher, F.; Geier, J.; Böhler, C.; Rüegger, H.; Schönberg, H.; Grützmacher, H. *Chem. Eur. J.* **2004**, *10*, 4198.

(6) Briceño, A.; Dorta, R. *Acta Crystallogr.* **2007**, *E63*, m1718.

(7) Defieber, C.; Ariger, M. A.; Moriel, P.; Carreira, E. M. *Angew. Chem., Int. Ed.* **2007**, *47*, 3139.

(8) (a) Takaya, Y.; Ogasawara, M.; Hayashi, T.; Sakai, M.; Miyaura, M. *J. Am. Chem. Soc.* **1998**, *120*, 5579. (b) Takaya, Y.; Ogasawara, M.; Hayashi, T. *Chirality* **2000**, *12*, 469. (c) Reetz, M. T.; Moulin, D.; Gosberg, A. *Org. Lett.* **2001**, *3*, 4083. (d) Mariz, R.; Luan, X.; Gatti, M.; Linden, A.; Dorta, R. *J. Am. Chem. Soc.* **2008**, *130*, 2172. (e) Burgi, J. J.; Mariz, R.; Gatti, M.; Drinkel, E.; Luan, X. J.; Blumentritt, S.; Linden, A.; Dorta, R. *Angew. Chem., Int. Ed.* **2009**, *48*, 2768. (f) Chen, J.; Chen, J.; Lang, F.; Zhang, X.; Cun, L.; Zhu, J.; Deng, J.; Liao, J. *J. Am. Chem. Soc.* **2010**, *132*, 4552.

(9) (a) Boiteau, J.-G.; Imbos, R.; Minnaard, A. J.; Feringa, B. L. *Org. Lett.* **2003**, *5*, 681. (b) Boiteau, J.-G.; Imbos, R.; Minnaard, A. J.; Feringa, B. L. *J. Org. Chem.* **2003**, *68*, 9481. (c) Kurihara, K; Sugishita, N.; Oshita, K.; Piao, D.; Yamamoto, Y.; Miyaura, N. *J. Organomet. Chem.* **2007**, *692*, 428.

Published on Web 04/30/2010

Chart 1. Chiral P-Alkene Ligands Based on the Tropylidene and Dibenz[*b*,*f*]azepine Moieties

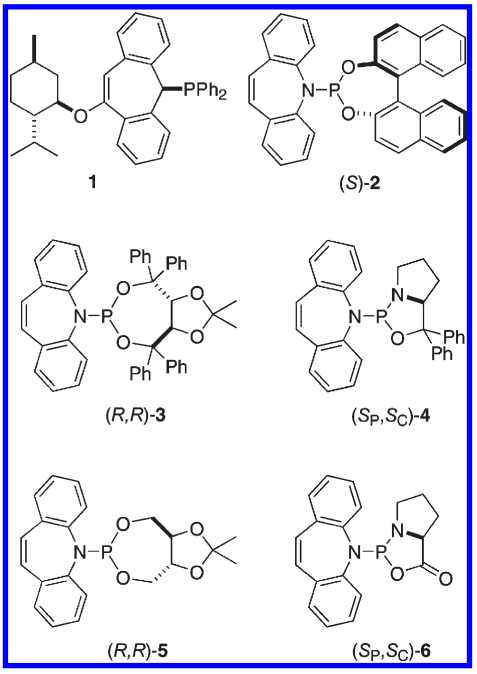

phosphine−olefin ligands[11] and phosphoramidite-alkene ligands such as **2**−**6**.[1] These latter ligands formed dinuclear chloro-bridged Rh complexes (of type **7**; see Scheme 1), and their bidentate coordination mode was authenticated by X-ray crystallography. The solid-state structures of ligands and complexes revealed a hybridization change of the dibenz[*b*,*f*]azepine N atom from sp^2 in the free ligands to sp^3 in the bidentate complexes, and we anticipated that this kind of spring-loaded coordination in combination with the comparatively weak metal−alkene interaction might favor ligand hemilability.[12] Hemilabile ligands are important in catalysis because they stabilize resting states while freeing up coordination sites when they are needed, thus assuming the role of a coordinating solvent.[13] Recently, Mezzetti and co-workers pointed out that the classic Feringa type "monodentate" phosphoramidites actually augment their hapticity through secondary, hemilabile interactions of their aryl functions with the metal center,[14] and chiral hemilabile amido-phosphines were shown to be excellent ligands for

Scheme 1

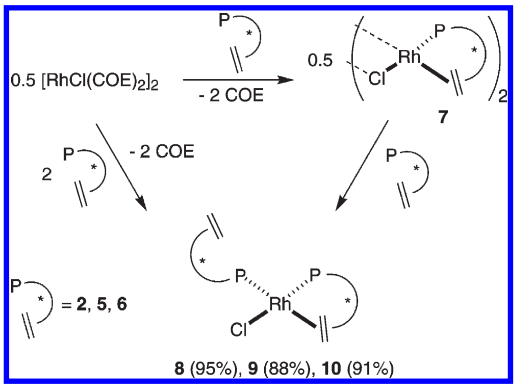

the Rh-catalyzed CAs of arylboronic acids.[15] In this context we note that Hayashi et al. postulated a solvent-stabilized 14-valence-electron intermediate ([Rh(OH)(S)(binap)], S = 1,4-dioxane) in the catalytic cycle of the CA of phenylboronic acid to methyl vinyl ketone. The intermediate is thought to form upon breakage of the hydroxo bridges of the complex $[Rh(\mu\text{-OH})(binap)]_2$.[16] Analogously, having potentially hemilabile P-alkene ligands at hand, our working hypothesis is based on the alkene-stabilized mononuclear hydroxo complex [Rh(OH)(κ^1P-alkene)(κ^2P-alkene)] representing the resting state of the active 14-electron species [Rh(OH)(κ^1P-alkene)(κ^1P-alkene)]. Thus, catalyst precursors of the composition Rh(P-alkene)$_2$X seem to be a worthwhile synthetic goal.

Chiral Cu−phosphoramidite complexes represent the alternative of choice for CA reactions when dialkylzinc[17] and trialkylaluminum[18] nucleophiles are to be used. Chiral Cu phosphoramidite complexes are usually prepared in situ, and the optimal ligand to Cu ratio was determined to be 2. However, due to dynamic processes in solution several species may form exhibiting varying Cu/ligand stoichiometries and coordination geometries.[19] Bis-phosphoramidite Cu−bromide complexes $[Cu(\mu\text{-Br})(L)_2]_2$ were shown to be dimeric in the crystal,[20] and although Feringa and co-workers were able to structurally characterize a monomeric phosphoramidite Cu complex of composition $[Cu(I)(L)_3]$,[17a] it does not represent a catalytically relevant species in CA reactions due to its ligand/Cu stoichiometry of 3.[17b] We reasoned that the use of phosphoramidite-alkene ligands **2**−**6** may stabilize corresponding Cu(I) complexes of the correct stoichiometry through secondary interactions of the alkene function and thus lead to isolable and well-defined systems.

In this paper we describe the synthesis of chiral mononuclear Rh(I) complexes of the composition Rh(P-alkene)$_2$X bearing ligands **2**, **5**, and **6**, which are shown to be hemilabile. We also show that mononuclear Cu(I) complexes

(10) (a) Hayashi, T.; Ueyama, K.; Tokunaga, N.; Yoshida, K. *J. Am. Chem. Soc.* **2003**, *125*, 11508. (b) Tokunaga, N.; Otomaru, Y.; Okamoto, K.; Ueyama, K.; Shintani, R.; Hayashi, T. *J. Am. Chem. Soc.* **2004**, *126*, 13584. (c) Defieber, C.; Paquin, J.-F.; Serna, S.; Carreira, E. M. *Org. Lett.* **2004**, *6*, 3873. (d) Shintani, R.; Okamoto, K.; Otomaru, Y.; Ueyama, K.; Hayashi, T. *J. Am. Chem. Soc.* **2005**, *127*, 54. (e) Paquin, J. F.; Stephenson, C. R. J.; Defieber, C.; Carreira, E. M. *Org. Lett.* **2005**, *7*, 3821. (f) Paquin, J.-F.; Defieber, C.; Stephenson, C. R. J.; Carreira, E. M. *J. Am. Chem. Soc.* **2005**, *127*, 10850. (g) Otomaru, Y.; Kina, A.; Shintani, R.; Hayashi, T. *Tetrahedron: Asymmetry* **2005**, *16*, 1673. (h) Otomaru, Y.; Okamoto, K.; Shintani, R.; Hayashi, T. *J. Org. Chem.* **2005**, *70*, 2503.

(11) Duan, W.-L.; Iwamura, H.; Shintani, R.; Hayashi, T. *J. Am. Chem. Soc.* **2007**, *129*, 2130.

(12) In related studies we observed that the alkene function of **2**−**6** does not coordinate to Pd(II) (unpublished results and ref 6).

(13) Jeffrey, J. C.; Rauchfuss, T. B. *Inorg. Chem.* **1979**, *18*, 2658. For uses of hemilabile ligands in industrial catalysis, see: (a) Parshall, G. W.; Ittel, S. D. *Homogeneous Catalysis: The Applications and Chemistry of Catalysis by Soluble Transition Metal Complexes*, 2nd ed.; Wiley-Interscience: New York, 1992; pp 70−72. (b) Keim, W. *Angew. Chem., Int. Ed.* **1990**, *29*, 235.

(14) Mikhel, I. S.; Rüegger, H.; Butti, P.; Camponovo, F.; Huber, D.; Mezzetti, A. *Organometallics* **2008**, *27*, 2937.

(15) (a) Kuriyama, M.; Tomioka, K. *Tetrahedron Lett.* **2001**, *42*, 921. (b) Kuriyama, M.; Nagai, K.; Yamada, K.-I.; Miwa, Y.; Taga, T.; Tomioka, K. *J. Am. Chem. Soc.* **2002**, *124*, 8932.

(16) Kina, A.; Iwamura, H.; Hayashi, T. *J. Am. Chem. Soc.* **2006**, *128*, 3904.

(17) (a) De Vries, A. H.; Meetsma, A.; Feringa, B. L. *Angew. Chem.* **1996**, *108*, 2526. (b) Alexakis, A.; Benhaim, C.; Rosset, S.; Humam, M. *J. Am. Chem. Soc.* **2002**, *124*, 5262.

(18) (a) D'Augustin, M.; Palais, L.; Alexakis, A. *Angew. Chem., Int. Ed.* **2005**, *44*, 1376. (b) Alexakis, A.; Albrow, V.; Biswas, K.; D'Augustin, M.; Prieto, O.; Woodward, S. *Chem. Commun.* **2005**, 2843.

(19) Zhang, H.; Gschwind, R. M. *Angew. Chem., Int. Ed.* **2006**, *45*, 6391.

(20) Shi, W.-J.; Wang, L.-X.; Fu, Y.; Zhu, S.-F.; Zhou, Q.-L. *Tertrahedron: Asymmetry* **2003**, *14*, 3867.

Chart 2

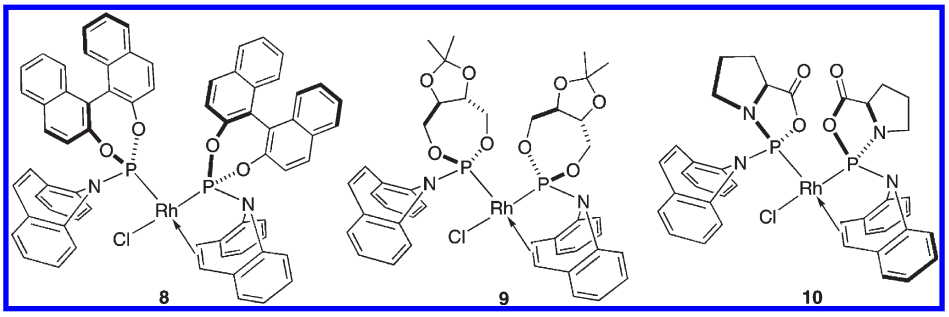

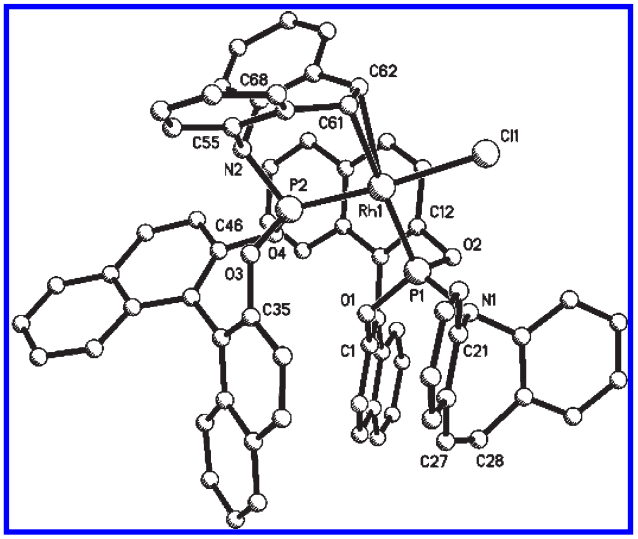

Figure 1. Structure of complex **8** in the crystal. Selected bond lengths (Å) and angles (deg): Rh1−P1, 2.2421(16); Rh1−P2, 2.1464(16); Rh1−C61, 2.2296(6); Rh1−C62, 2.253(6); Rh1−Cl1, 2.4027(16); P1−N1, 1.661(5); P1−O1, 1.616(4); P1−O2, 1.614(4); P2−N2, 1.703(5); P2−O3, 1.624(4), P2−O4, 1.608(4); O1−C1, 1.391(6); O2−C12, 1.425(6); O3−C35, 1.398(6); O4−C46, 1.411(6); N1−C21, 1.430(7); N1−C34, 1.450(7); N2−C55, 1.440(7); N2−C68, 1.476(6); C27−C28, 1.318(8); C61−C62, 1.405(9); P1−Rh1−P2, 95.59(5); P1−Rh1−Cl1, 86.75(6); O2−P1−O1, 101.76(18); O2−P1−N1, 99.0(2); O1−P1−N1, 108.8(2); O4−P2−O3, 103.63(18); O4−P2−N2, 103.5(2); O3−P2−N2, 95.5(2); C21−N1−C34, 115.7(4); C21−N1−P1, 118.4(4); C34−N1−P1, 125.4(4); C55−N2−C68, 111.8(4); C55−N2−P2, 113.2(4); C68−N2−P2, 113.1(3).

with the sought-after L:Cu ratio of 2 are accessible with ligands **2**, **4**, and **5**. We then find that these mononuclear complexes catalyze the asymmetric 1,4-addition of carbon nucleophiles to enones with enantioselectivities of up to 99% ee.

Results and Discussion

1. Complex Syntheses. In the course of our studies on the formation of dinuclear chloro-bridged Rh(I) complexes of type **7** (see Scheme 1) with chiral P-alkene ligands starting from $[RhCl(COE)_2]_2$ (COE = cyclooctene), we sometimes observed the formation of a byproduct consisting of mononuclear species such as **8** when care was not taken to *slowly* add the ligand to the Rh precursor. Four equivalents of binaphthol-derived ligand **2** cleanly reacted with $[RhCl(COE)_2]_2$ to form 2 equiv of $[RhCl(\mathbf{2})_2]$ (**8**; Chart 2) on a gram scale in almost quantitative yield. This bright orange complex was only sparingly soluble in common solvents, and its $^{31}P\{^1H\}$ NMR spectrum suggested cis coordination of the P atoms: two doublets of doublets are centered at 120 and 179 ppm (P atom trans to Cl) with $J_{RhP} = 286$ Hz, $J_{RhP'} = 283$ Hz, and $J_{PP'} = 45$ Hz.

Table 1. Torsion Angles in 2 and 6 along Their P−N Bonds[a] as a Function of Coordination Mode

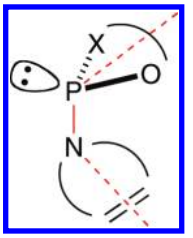

ligand	**2** (X = O)	**6** (X = N)
free	−116.68(2)[b]	−99.32(1)[b]
monodentate	−51.309(24)[c]	41.715(4)[d]
bidentate	172.29(11)[c]	176.97(2)[d]

[a] For definitions of centroids, see the text. [b] Taken from ref 1. [c] Complex **8**. [d] Complex **10**.

X-ray-quality single crystals of **8** were obtained from CH_3CN, and a diffraction study confirmed the expected cis coordination of the phosphorus atoms in a pseudo-square-planar coordination environment (see Figure 1 and Table 5 for crystal data and collection parameters). This structure allowed us to directly compare the structural variations of the mono- and bidentate coordination modes of ligand **2** within the same metal complex. (1) The uncoordinated alkene arm displays a C27−C28 distance of 1.318(8) Å, which is shorter than the C7−C8 distance of 1.405(9) Å in its coordinated counterpart. (2) While the N1 atom of the monodentate ligand is nearly planar, with a deviation of only −0.062(6) Å with respect to the plane formed by its substituents P1/C21/C34 (similar to the value found in the free ligand **2**),[1] the N2 atom in the bidentate ligand adopts a pyramidal geometry with a deviation of 0.423(6) Å in relation to the P2/C55/C68 plane. (3) The torsion angle along the P−N vector of ligand **2** is strongly dependent on its coordination mode (see Table 1). We measure this torsion angle by connecting the centroid of the alkene function of the dibenz[*b*,*f*]azepine moiety to its N atom and by connecting the P atom to the centroid of the C−C bond joining the two naphthyl units, as illustrated by the red dotted lines in the drawing of Table 1. Structure **8** shows that ligand **2** in its bidentate ligand mode adopts a nearly perfect (i.e., 180°) anti conformation, with a torsion angle of 172.29(11)°

along Centr1(C61−C62)−N2−P2−Centr2(C44−C45). In its monodentate mode, ligand **2** displays a syn conformation with a torsion angle of −51.309(24)° along Cent1(C44−C45)−N1−P1−Cent2(C10−C11). This means that the uncoordinated alkene centroid is tilted away by ca. 136° in comparison to its coordinated counterpart. The torsional conformation of the free ligand **2** in the crystal lies between the values of mono- and bidentate **2**. The C1−C10−C11−C12 and C35−C44−C45−C46 torsion angles of the naphthyl groups are ca. 52° in both cases and fall into the usual range.

The taddol-derived ligand **3** behaved quite differently, and even large excesses of **3** in combination with either $[RhCl(COE)_2]_2$ or $[RhCl(COD)]_2$ (COD = 1,5-cyclooctadiene) did not lead to the formation of the sought-after complex $[RhCl(\mathbf{3})_2]$ but only afforded the dimer $[RhCl(\mathbf{3})]_2$[1] along with unreacted ligand. Similarly, the addition of 4 equiv of diphenylprolinol-derived ligand **4** to $[RhCl(COE)_2]_2$ only led to an inseparable mixture of the minor (27% of total P integrals) expected complex $[RhCl(\mathbf{4})_2]$ and a major fluxional species that was observed in situ by NMR spectroscopy. The reluctance of ligands **3** and **4** to coordinate in a 2:1 stoichiometry is possibly due to the steric bulk exerted by the phenyl groups present in both ligands. Indeed, complex **9**, bearing the less bulky analogue of ligand **3**, was obtained in good yield by adding 4 equiv of ligand **5** to $[RhCl(COE)_2]_2$ and its $^{31}P\{^1H\}$ NMR spectrum showed the characteristic pattern already observed with complex **8** indicative of cis coordination of the P atoms (two doublets of doublets centered at 121 and 151 ppm with J_{RhP} = 275 Hz, $J_{RhP'}$ = 267 Hz, and $J_{PP'}$ = 52 Hz).

Likewise, by lowering the steric pressure exerted by the diphenylprolinol auxiliary in ligand **4** and instead using the simple proline-derived analogue **6**, the complex $[RhCl(\mathbf{6})_2]$ (**10**; see Chart 2) formed in excellent yields either from $[RhCl(COE)_2]_2$ or from the more convenient starting material $[RhCl(COD)]_2$ by displacement of the COD molecule.[21] As for complexes **8** and **9**, the $^{31}P\{^1H\}$ NMR spectrum **10** suggested cis coordination of the P atoms with doublets of doublets at 135 ppm (J_{RhP} = 258 Hz, $J_{PP'}$ = 59.5 Hz) and at 176 ppm (J_{RhP} = 250 Hz, $J_{PP'}$ = 59.5 Hz). The precise molecular structure of complex **10** was revealed by a single-crystal diffraction analysis and is depicted in Figure 2.

In analogy to the structure of **8**, complex **10** features cis coordination of the P atoms in a pseudo-square-planar coordination environment. The distances of 1.337(8) Å for the uncoordinated C26−C27 alkene arm and of 1.389(7) Å for the coordinated C7−C8 counterpart are similar to those observed in compound **8**. The monodentate ligand **6** shows a syn conformation of the dibenz[*b*,*f*]azepine moiety and the proline ring with a torsion angle of 41.7° along the P1−N1 vector (defined in analogy to complex **8**, i.e. Cent1-(C26−C27)−N3−P2−Cent2(C37−C38); see Table 1). On the other hand, ligand **6** in a bidentate coordination mode exhibits an almost perfect anti conformation with a torsion angle of 177.0°, along Cent1(C7−C8)−N1−P1−Cent2-(C18−C19). Thus, the alkene centroid turns by ca. 136° between the mono- and bidentate coordination modes, the same amount as in complex **8** (see above). Again, the free

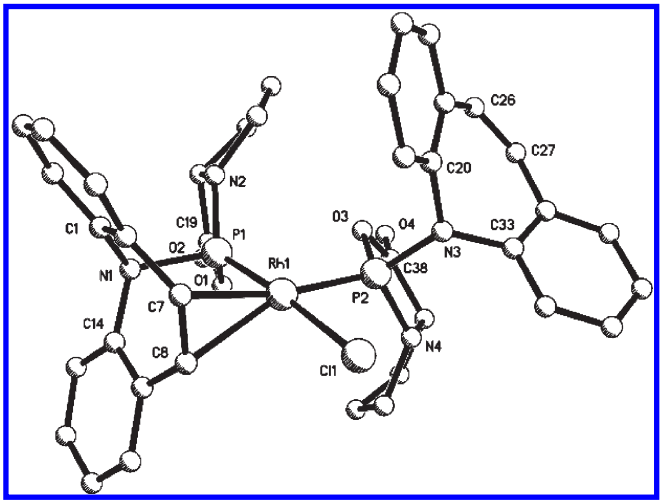

Figure 2. Structure of complex **10** in the crystal. Selected bond lengths (Å) and angles (deg): Rh1−P1, 2.1385(14); Rh1−P2, 2.2107(14); Rh1−C7, 2.309(5); Rh1−C8, 2.286(4); Rh1−Cl1, 2.3957(14); P1−N1, 1.723(4); P1−N2, 1.638(4); P1−O1, 1.657(3); P2−N4, 1.658(4); P2−N3, 1.659(4); P2−O3, 1.681(4), O1−C19, 1.368(6); O2−C19, 1.195(6); O4−C8, 1.198(7); O3−C38, 1.376(7); N1−C1, 1.454(6); N1−C14, 1.451(6); N3−C20, 1.456(6); N3−C33, 1.435(6); C7−C8, 1.389(7); C26−C27, 1.337(8); P1−Rh1−P2, 92.94; P1−Rh1−Cl1, 175.47(6); C1−N1−C14, 114.6(4); C14−N1−P1, 113.1(3); C1−N1−P1, 109.7(3); C33−N3−C20, 116.2(4); C33−N3−P2, 122.7(3), C20−N3−P2, 119.4(3).

ligand **6** in its crystalline state adopts a conformation that lies between the two coordination modes. The dihedral angles between the five-membered rings are 118° for the monodentate ligand and 136° for the bidentate ligand. As in structure **8**, the N3 atom of the monodentate ligand is nearly planar with a deviation of −0.113(5) Å with respect to the plane formed by the P2/C33/C20 atoms (similar to the value found in the free ligand **6**),[1] while the N1 atom in the bidentate ligand adopts a trigonal-pyramidal geometry with a deviation of 0.429(5) Å with respect to the P1/C1/C14 plane. We also note that the P−O and P−N distances contract slightly when compared to the distances in the free ligand **6**.[1]

Complexes **8**−**10** were appreciably soluble in chlorinated solvents, affording orange solutions, while in benzene, toluene, THF, CH_3CN, and NEt_3 they were only sparingly soluble. In methanol decomposition of complex **10** took place at 333 K. On the other hand, **8** and **10** dissolved readily in pyridine-d_5 to give yellow solutions and their NMR spectra indicated the generation of solvated species (see eq 1): the $^{31}P\{^1H\}$ NMR spectrum of solvated **8**·py showed a pair of broad doublets of doublets centered around 144 and 150 ppm with J_{RhP} = 306 Hz and $J_{RhP'}$ = 264 Hz, respectively ($J_{PP'}$ = 57 Hz), and **10**·py displayed a very similar pair of broad doublets of doublets at 149 and 156 ppm with J_{RhP} = 279 Hz and $J_{RhP'}$ = 238 Hz, respectively ($J_{PP'}$ = 48 Hz). The lemon yellow pyridine adduct **8**·py crystallized from its pyridine solution by exposure to Et_2O vapor.[22] However, this microcrystalline product slowly lost solvent when left open to the glovebox atmosphere, and vacuum treatment mostly yielded the

(21) The originally targeted complex [Rh(**6**)Cl(COD)] was never isolated in pure form, the main contaminant being the 1:2 complex **10** even when the $[RhCl(COD)]_2$:**6** stoichiometry was strictly kept as 1:1 and the ligand was added slowly to the Rh precursor.

(22) Anal. Found: C, 70.00; H, 3.98; N, 3.37; Calcd for **8**·py·H_2O (hygroscopic!): C, 70.11; H, 4.11; N, 3.36.

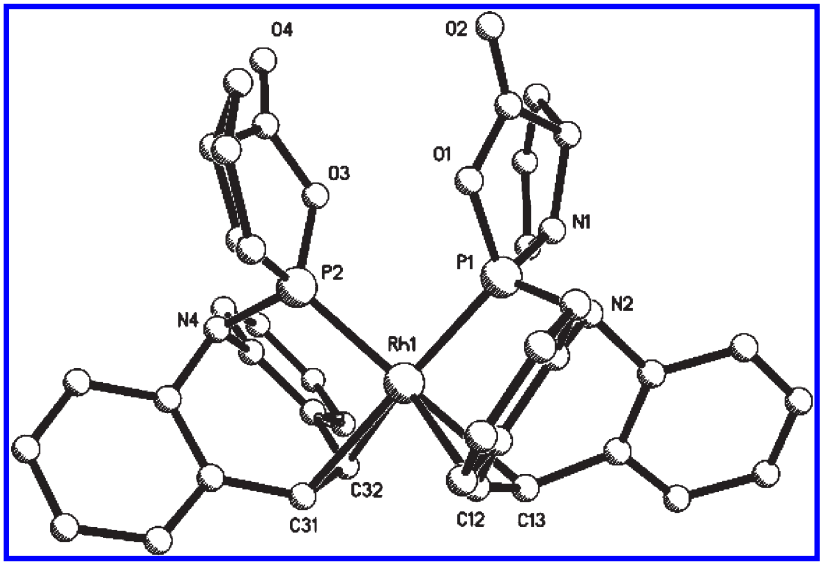

Figure 3. Structure of the cation of **12** in the crystal. Selected bond lengths (Å) and angles (deg): Rh1−P1, 2.185(2); Rh1−P2, 2.184(2); Rh1−C12, 2.320(8); Rh1−C13, 2.385(7); Rh1−C31, 2.359(8); Rh1−C32, 2.38524(9); P1−N1, 1.640(8); P1−N2, 1.703(7); P1−O1, 1.656(6); P2−N3, 1.638(9); P2−N4, 1.715(8); P2−O3, 1.641(6); N2−C6, 1.460(10); N2−C19, 1.449(11); N4−C25, 1.447(12); N4−C38, 1.477(14); C12−C13, 1.391(16); C31−C32, 1.383(14); P1−Rh1−P2, 92.52(9); C6−N2−P1, 111.4(5); C19−N2−P1, 112.5(5); C19−N2−C6, 113.2(7); C25−N4−C38, 114.5(8); C25−N4−P2, 109.5(7), C38−N4−P2, 112.2(6).

orange starting complex **8**, thus clearly indicating the reversibility of solvent coordination.[23]

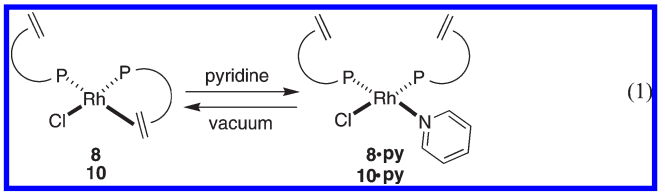

(1)

Complexes **8** and **10** were transformed to the respective tetrafluoroborate salts **11** and **12** in excellent yields according to Scheme 2.[24] While the starting chloride complexes in solution are orange or dark yellow, their cationic counterparts **11** and **12** form deep red solutions.[25] The $^{31}P\{^{1}H\}$ NMR spectra of the cations are simplified to one characteristic sharp doublet resonating at 165.7 ppm (J_{RhP} = 280 Hz) and at 161.5 ppm (J_{RhP} = 256 Hz), respectively, indicative of the higher symmetry of the cations and pointing to a cis arrangement of the ligands. Trans coordination of the chiral ligands would lead to complexes of lower symmetry and correspondingly complex $^{31}P\{^{1}H\}$ NMR spectra. In fact, similar complexes having trans geometry and high symmetry (with the Rh atom lying on a center of inversion) were described with achiral P-alkene ligands.[4a] The addition of 1 equiv of the

Scheme 2

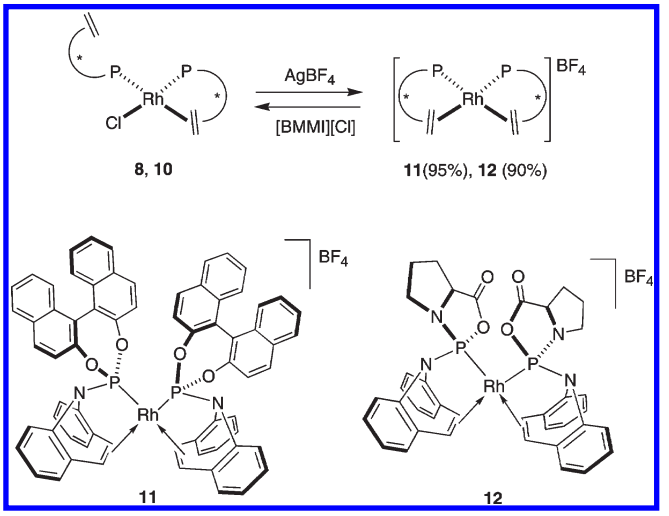

CD_2Cl_2-soluble 1-butyl-2,3-dimethylimidazolium chloride ([BMMI][Cl]) to the red cationic complexes **11** and **12** quantitatively regenerated within the time of mixing the neutral yellow species **8** and **10** (Scheme 2).

The X-ray crystal structure of complex **12**, bearing the proline-derived ligand, confirmed the cis orientation of the two ligands in a pseudo-square-planar coordination environment and the pseudo-C_2 point symmetry of the cation (see Figure 3). The distances of the coordinated alkene functions C12−C13 and C31−C32 are 1.391(16) and 1.383(14) Å, respectively, and are statistically equal to those observed in the neutral complexes **8** and **10**. Likewise, both nitrogen atoms N2 and N4 of the dibenz[*b*,*f*]azepine moieties adopt a pyramidal geometry with deviations of −0.431(8) and −0.442(9) Å in relation to the P1/C6/C19 and P2/C25/C38 planes, respectively.

Similarly to the addition of Cl^- to the cations **11** and **12** (Scheme 2), excess amounts of pyridine, CH_3CN, or DMSO

(23) The quantification of these equilibria is the subject of ongoing studies. Heating a solution of complex **9** in a "noncoordinating" solvent such as toluene-d_8 at 373 K caused the dd at 122 ppm in the $^{31}P\{^{1}H\}$ NMR spectrum that corresponds to the P atom trans to the alkene to broaden to a considerably larger extent than the signal of the P atom trans to the chloride ligand. This observation suggests a hemilabile alkene coordination stabilizing a 14-electron species.

(24) **12** also formed quantitatively by disproportionation when $AgBF_4$ was added to a mixture of 0.5 equiv of $[RhCl(COD)]_2$ and **2** in an attempt to synthesize [Rh(**2**)(COD)]BF_4.

(25) The reaction of **10** with 1 equiv of $AgBF_4$ in THF solution yields a light-stable and isolable brick red Ag adduct (in CH_2Cl_2 AgCl precipitates out to liberate the silver-free complex **12**; see the Experimental Section). We speculate that in THF AgCl is complexed by the two carbonyl teeth of the proline moiety (see Figure 3, work in progress).

Scheme 3. Solvation Equilibria of 11 with S = Pyridine, CH_3CN, DMSO and Their Isolated Analogues 13 and 14

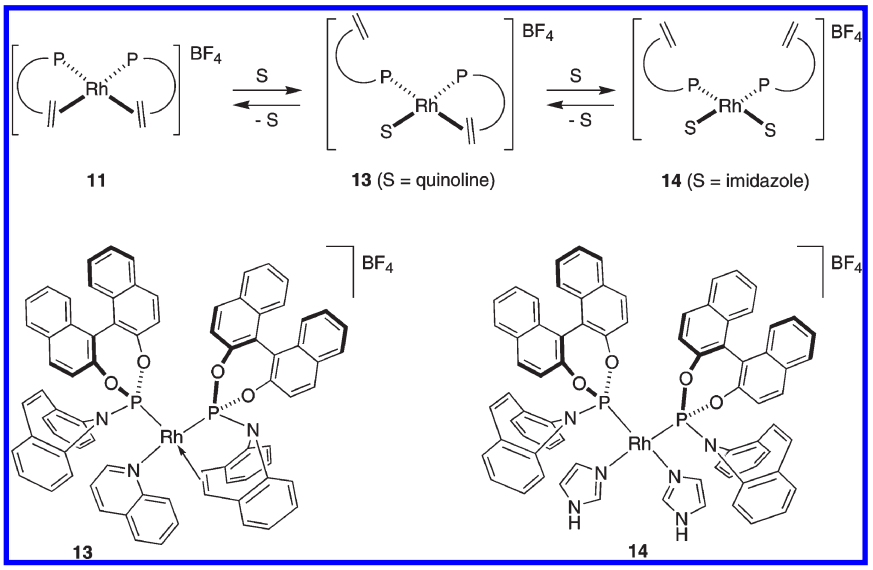

to the blood red solutions of **11** and **12** led to lemon yellow solutions by the time of mixing. Even though these cationic solvento complexes (analogues of **14**; see Scheme 3) were more stable than the corresponding neutral chlorides **8**·py and **10**·py described above, they were not readily amenable to isolation. These adducts did not withstand vacuum drying or washings with pentane or Et_2O, thereby successively losing the coordinated solvent molecules and reverting first to the monosolvento complex **13** (observed in situ by $^{31}P\{^1H\}$ NMR) and finally to the starting dark red Rh cation **11** according to Scheme 3. However, the heavier and bulkier pyridine analogue quinoline readily coordinated to **11**, allowing the isolation and characterization of the orange monosolvento complex **13**. This high-yielding reaction was completely selective for the 1:1 adduct, and even at a 10-fold excess of quinoline, no bis-solvento analogue was observed. Neither under high vacuum nor on washing **13** with alkanes or ether did we observe decoordination of the quinoline molecule. Its $^{31}P\{^1H\}$ NMR spectrum indicated lowered symmetry with respect to **11**, showing a pair of doublets of doublets centered at 116 ppm (J_{RhP} = 299 Hz, $J_{PP'}$ = 59 Hz) and 182 ppm ($J_{RhP'}$ = 246 Hz, $J_{PP'}$ = 59 Hz), reminiscent of the spectrum of the chloride complex **8**. Similarly, in an attempt to model the bis-solvento complex we opted for imidazole to mimic pyridine, due to its lower volatility and improved crystallinity. Indeed, addition of 2 equiv of imidazole to **11** in CH_2Cl_2 solution yielded the bis-imidazole adduct **14** almost quantitatively as a lemon yellow, microcrystalline powder. As expected, the $^{31}P\{^1H\}$ NMR spectrum indicated higher symmetry, featuring a sole broadened doublet at 148 ppm (J_{RhP} = 273 Hz), similar to the spectrum of **11**, and the imidazole protons were characterized by a broad singlet at 11.6 ppm in the ^1H NMR spectrum. However, electron spray ionization of **13** and **14** in a CH_3CN matrix only gave the molecular peak of the cation of **11** in both cases. Additions of other nucleophiles to cations **11** and **12** that are relevant to CA catalysis such as hydroxides and arylboronic acids only led to inseparable mixtures.

The neutral Cu(I) iodide complexes **15**−**17** were prepared on gram scales by adding benzene to CuI and 2 equiv of ligands **2**, **4**, and **5**, respectively (see eq 2). $^{31}P\{^1H\}$ NMR spectra of all three complexes showed broad singlets ($\nu_{1/2} \approx$ 80 Hz). When only 1 equiv of ligand **2** was reacted slowly with CuI in benzene solution, the 1:2 adduct **15** formed along with 0.5 equiv of unreacted CuI.[26] ^1H NMR spectra of compounds **15**−**17** did not indicate coordination of the olefin functions of ligands **2**, **4**, and **5** to the Cu center, and the monodentate coordination mode was confirmed by X-ray single-crystal diffraction experiments on complexes **15** and **16** (see Figures 4 and 5 and Table 5 for crystal data and diffraction parameters). Both complexes are monomeric with a trigonal-planar coordination around the Cu atom.[27]

The asymmetrical unit of **15** contains half of the neutral complex that displays C_2 symmetry along the Cu−I vector. The N atom of the dibenzazepine moiety adopts a trigonal-planar conformation with a deviation of −0.078(9) Å in relation to the P1/C34/C21 plane. The dibenzazepine unit was found disordered over two sets of positions (see Crystal Structure Determinations). The torsion angle of the naphthyl groups along C1−C10−C11−C12 is ca. 50°. In contrast, the asymmetrical unit of **16** contains a complete molecular unit, which also exhibits a pseudo-C_2 symmetry around the Cu−I bond. Similar planar conformations of N2 and N4 are observed with distances of 0.149(8) and 0.067(8) Å from the P1/C18/C31 and P2/C49/C62 planes, respectively.

In order to assess the coordinating ability of the olefinic part of the ligands in complexes **15** and **16**, the iodide was abstracted with $AgBF_4$ in THF solution to afford the two new complexes **18** and **19**, respectively, in excellent yields according to eq 2. Their $^{31}P\{^1H\}$ NMR spectra showed small low-field frequency shifts compared to the iodides, while the ^1H NMR spectra did not provide evidence for olefin coordination to the Cu centers. Large single crystals of **18** were grown from a saturated and filtered toluene solution. Unfortunately, attempts to solve the crystal

(26) Three equivalents of ligand **6** reacted with CuI to form a complex displaying a broad singlet at around 122 ppm in the $^{31}P\{^1H\}$ NMR spectrum.

(27) For an example of a structurally characterized chiral monomeric Cu diphosphine complex used in CA of Grignard nucleophiles, see: López, F.; Harutyunyan, S. R.; Meetsma, A.; Minnaard, A.; Feringa, B. L. *Angew. Chem., Int. Ed.* **2005**, *44*, 2752.

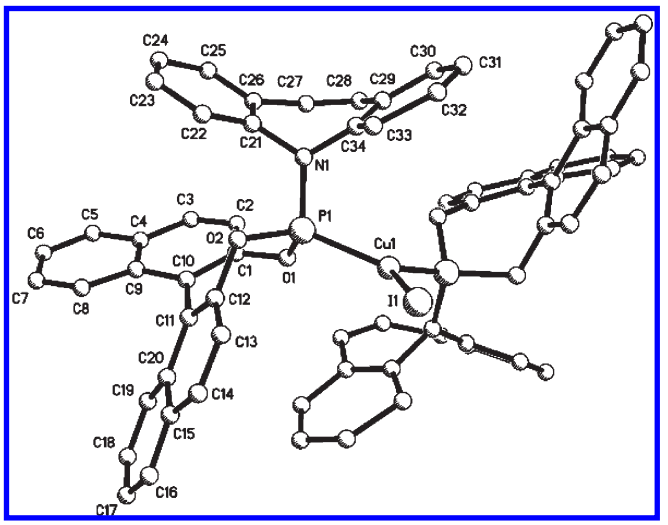

Figure 4. Structure of complex **15** in the crystal showing the C_2 symmetry around the Cu−I vector. Selected bond lengths (Å) and angles (deg): I1−Cu1, 2.4983(12); Cu1−P1, 2.2294(18); N1−C34, 1.391(8); N1−C21, 1.443(8); N1−P1, 1.661(6); P1−O1, 1.619(4); P1−O2, 1.637(4); O1−C1, 1.391(7); O2−C12, 1.412(7); C27−C28, 1.317(5); P1−Cu1−P1^{i}, 109.18(9); P1−Cu1−I1, 125.41(4); P1^{i}−Cu1−I1, 125.41(4); C34−N1−P1, 117.8(9); C21−N1−P1, 122.3(6); C34−N1−C21, 119.0(10); Symmetry code: (*i*) $-x+2, -y+2, z$.

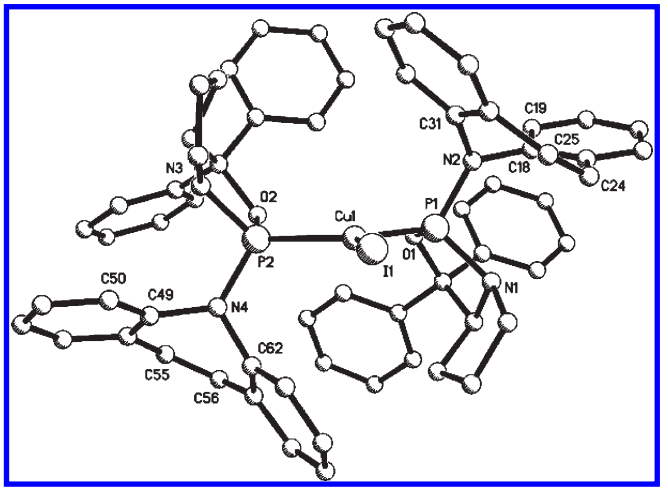

Figure 5. Structure of complex **16** in the crystal. Selected bond lengths (Å) and angles (deg): Cu1−I1, 2.5354(13); Cu1−P1, 2.246(2); Cu1−P2, 2.255(2); P1−N1, 1.698(6); P1−N2, 1.663(7); P1−O1, 1.627(5); P2−N3, 1.682(7); P2−N4, 1.672(7); P2−O2, 1.617(5); N1−C2, 1.470(10); N1−C5, 1.481(10); N2−C18, 1.439(10); N2−C31, 1.443(9); N3−C33, 1.442(10); N3−C36, 1.471(11); N4−C49, 1.461(11); N4−C62, 1.454(10); C55−C56, 1.345(15); C24−C25, 1.339(14); P1−Cu1−P2, 120.82(9); P1−Cu1−I1, 120.90(7); O1−P1−N1, 93.2(3); O1−P1−N2, 107.7(3); N2−P1−N1, 104.9(3); O2−P2−N3, 93.2(3); O2−P2−N4, 110.4(3); N4−P2−N3, 102.7(3); C18−N2−P1, 125.4(5); C31−N2−P1, 118.5(6); C18−N2−C31, 113.2(6); C62−N4−C49, 112.7(6); C62−N4−P2, 120.2(5); C49−N4−P2, 126.5(6).

structure were hampered by serious disorder.[28] At least two comments about the structure may be made at this stage: First, the alkene functions of the two ligands do not coordinate the Cu center, and second, the coordination sphere around Cu is trigonal planar. We believe that the third coordination site is occupied by the BF_4 counteranion as depicted in the proposed structure[29] in eq 2. However, THF instead of anion coordination cannot be ruled out on the basis of the available diffraction data. The most obvious difference in the coordination modes of the P-alkene ligands on comparison of the Rh(I) and Cu(I) complexes is the absence of alkene binding to Cu(I), to the extent where the weakly coordinating anion BF_4^- appears to be the preferred ligand. This could be explained by the preference of the P-alkene ligands for smaller bite angles in square-planar complexes and a stronger alkene−Rh(I) interaction due to efficient metal−alkene back-bonding.

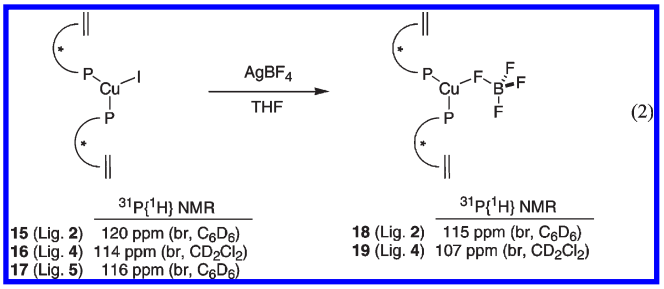

2. Catalysis. Preliminary trials showed the neutral monomeric Rh−chloride complexes **8** and **9** to be far more active catalysts for the CA of arylboronic acid nucleophiles to enones than the corresponding recently reported chloro-bridged dimeric Rh complexes of type **7** (vide supra).[1] For example, in the benchmark reaction of phenylboronic acid with cyclohexenone at 80 °C in a dioxane/H_2O/KOH mixture, the dimer [Rh(μ-Cl)(**2**)]$_2$ yielded 90% of 3-phenylhexanone after 1 h reaction time, while the corresponding monomer **8** gave quantitative yields in less than 0.5 h with similar selectivity.[30] We therefore chose a reaction temperature of 40 °C to compare the performance of complexes **8**−**14**, and the results are summarized in Table 2.

Complex **8** turned out to be quite an enantioselective catalyst, while **9**, bearing the less bulky taddol-derived ligand, was very active. The neutral complex **10** and cationic **12** bearing the proline-derived ligand **6** fared poorly. Apparently the ester function present in ligand **6** is incompatible with the phenylboronic acid substrate, which may also explain the formation of a black precipitate during catalysis. On the other hand, cation **11** combined excellent activity with high enantioselectivity and thus was used in the subsequent substrate screening (see Table 3). The high activity of **11** in comparison to its neutral analogue **8** could be explained by a swifter arylation and/or hydroxylation of the cationic Rh center during catalysis.[31] Since the quinoline and imidazole complexes **13** and **14** already contain bases, they were also tested in the absence of KOH; however, no reaction was

(28) Briceño, A.; Dorta, R. Unpublished data. Selected crystallographic parameters: $a = 14.0036$ Å, $b = 24.8871$ Å, $c = 10.6631$ Å, orthorhombic, space group $P2_12_12$, $V = 3716.2(4)$ Å^3, $Z = 2$.

(29) For structurally authenticated η^1 coordination of BF_4^- to Cu(I), see for example: Gandhi, B. A.; Green, O.; Burstyn, J. N. *Inorg. Chem.* **2007**, *46*, 3816.

(30) In comparison with the dimer [Rh(μ-Cl)(**2**)]$_2$, the presence of 2 equiv of ligand **2** per Rh metal in monomer **8** possibly slows catalyst decomposition and leads to a more favorable monomeric resting state.

(31) Miyaura and co-workers also noticed improved reactivity of cationic Rh species in such reactions.[9c] Furthermore, one of the reviewers suggested that the use of cationic species might be an important design element to optimize the performance of hemilabile ligand systems in general.

Table 2. Screening of Complexes 8−14 for the Catalytic 1,4-Addition

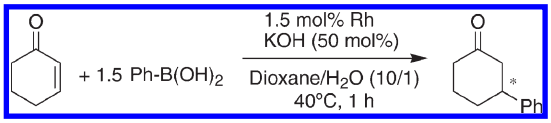

	catalyst						
	8	**9**	**10**	**11**	**12**	**13**	**14**
yield (%)[a]	33	83	38	93	trace	trace	33
ee (%)[b]	89	2	32	92	nd	nd	92
config[c]	*R*	*R*	*R*	*R*	nd	nd	*R*

[a] Isolated yields of 3-phenylcyclohexanone. [b] Determined by HPLC analysis with chiral column Daicel Chiralcel OD-H (for details see the Experimental Section). [c] Configuration determined by comparison with reported data. nd = not determined.

Table 3. Substrate Screening with Complex 11

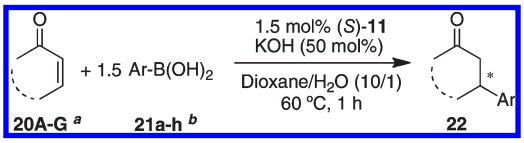

entry	enone[a]	boronic acid[b]	yield of **22** (%)[c]	ee (%)[d,e]
1	**20A**	**21a**	98 (**22Aa**)	88
2	**20A**	**21b**	98 (**22Ab**)	99
3	**20A**	**21c**	99 (**22Ac**)	99
4	**20A**	**21d**	98 (**22Ad**)	99
5	**20A**	**21e**	68 (**22Ae**)	99
6	**20A**	**21f**	55 (**22Af**)	85
7	**20A**	**21g**	75 (**22Ag**)	90
8	**20A**	**21h**	99 (**22Ah**)	95
9	**20B**	**21a**	90 (**22Ba**)	60
10	**20C**	**21a**	95 (**22Ca**)	95
11	**20D**	**21a**	90 (**22Da**)	99
12	**20E**	**21a**	97 (**22Ea**)	99
13	**20F**	**21a**	99 (**22Fa**)	98
14	**20G**	**21a**	60 (**22Ga**)	65

[a] Legend: **20A**, 2-cyclohexenone; **20B**, 2-cyclopentenone; **20C**, 3-penten-2-one; **20D**, 3-hepten-2-one; **20E**, 3-octen-2-one; **20F**, 3-nonen-2-one; **20G**, 5-methyl-3-hexen-2-one. [b] Ar = Ph (**21a**), 3-$CH_3C_6H_4$ (**21b**), 4-$CH_3C_6H_4$ (**21c**), 3-$CH_3OC_6H_4$ (**21d**), 4-FC_6H_4 (**21e**), 3-ClC_6H_4 (**21f**), 4-ClC_6H_4 (**21g**), 1-naphthyl (**21h**). [c] Isolated yields. [d] Determined by HPLC (chiral columns: Daicel Chiralcel OD-H, OJ-H, and OB; see the Experimental Section). [e] The major enantiomers all have the *R* configuration.

observed. Likewise, the quinoline adduct **13** in the presence of KOH did not exhibit any noticeable activity, while the imidazole complex **14** behaved like the neutral chloride analogue **8**.

The substrate screening reactions were performed at a slightly higher temperature of 60 °C, for it did not affect selectivities significantly (see entry 1, Table 3). The addition of a variety of arylboronic acids to cyclic and linear enones proceeded with very high activities and reaction times of less than 1 h. More importantly, enantioselectivities of the products were high and, at times, total stereocontrol was observed in the reaction employing complex **11** as the catalyst (entries 2−5, 11, and 12). Furthermore, all substrates were used from commercial suppliers as received without further purification, in order to test the robustness of the catalyst precursors toward common impurities.

Table 4. Screening of Complexes 15−19 for the Catalytic 1,4-Addition

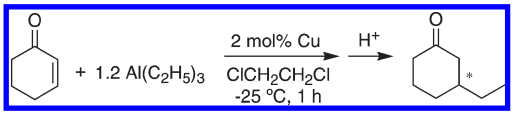

	catalyst					
		15	**16**	**17**	**18**	**19**
yield (%)[a]	64	52	24	47	98	98
ee (%)[b]	0	2	0	0	39	24
config[c]		*S*			*S*	*S*

[a] GC yields of 3-ethylcyclohexanone. [b] Determined by GC using a chiral Lipodex E column (for details see the Experimental Section). [c] Configuration determined by comparison with reported data.

The neutral Cu complexes **15**−**17** did not catalyze the ethylation of cyclohexenone with $AlEt_3$ in 1,2-dichloroethane solvent at −25 °C (see Table 4). It is noteworthy that the blank reaction afforded the 1,4-addition product in higher yield (64%) than in the presence of the Cu−iodo complexes **16**−**18**.[32] On the other hand, the corresponding cationic species **18** and **19** were active catalysts and, in the case of complex **18**, showed promising levels of enantioselectivity. The addition of $AlEt_3$ to the β-substituted enone 3-methyl-2-cyclohexenone was catalyzed by **18** at −25 °C and over 4 h to afford the quaternary ketone in 83% isolated yield and 9% ee. The optimization of these reactions is the subject of ongoing efforts in our laboratories.

Conclusions

Ligands **2**, **5**, and **6** were shown to act as hemilabile monodentate and bidentate ligands in mononuclear complexes of composition $RhX(L)_2$ (X = Cl, BF_4). The hemilabile nature of the alkene function in these ligands is in part due to a flexible hybridization state of the dibenz[*b*,*f*]azepine N atom, varying from quasi trigonal planar in the free and monodentate structures to pyramidal in bidentate structures with diminished P-alkene bite angles. The mononuclear complexes described here showed activities and selectivities for the CA of arylboronic acids to enones higher than those for the previously reported analogous neutral dimeric chloro-bridged complexes. In particular, the cationic mononuclear complex **11** turned out to be highly active and enantioselective, leading, in various cases, to optically pure cyclic and linear ketones in quantitative yields. These results highlight an often forgotten aspect in chiral catalyst development: optimization of catalyst performance may well be achieved by tuning the coordination sphere of the metal catalyst rather than by the usually less cost-effective strategy of ligand modification. Here we demonstrated a dramatic improvement of catalyst performance (using the same ligand!) simply by modifying the coordination chemistry of Rh(I) from dinuclear neutral to mononuclear cationic. Finally, ligands **2**, **4**, and **5** formed isolable complexes with CuI in a stoichiometry of 2:1 that is relevant to CA catalysis. Structural analyses only revealed monodentate P-coordination. The corresponding cationic species were active catalysts for the moderately enantioselective addition of $AlEt_3$ to cyclohexenone.

(32) Ashby, E. C.; Noding, S. A. *J. Org. Chem.* **1979**, *44*, 4792.

Experimental Section

All reactions were carried out under anaerobic and anhydrous conditions, using standard Schlenk and glovebox techniques, unless otherwise stated. Solvent distillation was carried out as follows: THF, Et_2O, and benzene from purple Na/Ph_2CO solutions; toluene from Na; pentane, C_6D_6, and THF-d_8 from Na_2K alloy; CH_3CN, CH_2Cl_2, and CD_2Cl_2 from CaH_2; NEt_3 and 1,4-dioxane from K. $CDCl_3$ was degassed with three freeze−pump−thaw cycles and then kept over activated molecular sieves (4 Å) in a glovebox. Quinoline (Merck) was distilled from a dark red Na solution. NMR spectra were recorded on a JEOL 400 MHz spectrometer. Ligands **2**−**6**,[1] [RhCl(COD)], and $[RhCl(COE)_2]_2$[33] were prepared according to published procedures. Only freshly precipitated, snow white CuI was used for complex synthesis. Only crystalline, *white* $AgBF_4$ was used (98%, Aldrich Corp.), and reactions involving Ag were carried out in the dark. Elemental analyses were performed at IVIC or OCI, and samples were handled in air (hygroscopic compounds are corrected for water content).

[RhCl((*S*)-2)$_2$] (8). Method A. A solution of **2** (1441.9 mg, 2.8071 mmol) in dioxane (30 mL) was added dropwise over 10 min to a vigorously stirred orange slurry of $[RhCl(COE)_2]_2$ (503.5 mg, 0.7071 mmol) in dioxane (30 mL) to afford a clear red solution that was stirred for 2 h. Then the volatiles were removed in vacuo and the solid was washed with hexane (2 × 40 mL). HV drying afforded 1.66 g (97%) of a fine orange powder. Anal. Found: C, 71.21; H, 4.03; N, 2.18. Calcd for $RhClC_{68}H_{44}N_2O_4P_2 \cdot {}^1/_3C_6H_{14}$: C, 71.12; H, 4.15; N, 2.37. ^{1}H NMR (400 MHz, $CDCl_3$): δ 4.84 (ABX, J = 56 Hz, 9 Hz, 2H), 6.10−6.20 (m, 2H), 6.40−7.75 (m, 35H), 7.80−7.85 (m, 1H), 7.90−8.10 (m, 2H), 8.25−8.30 (m, 1H), 8.80−8.85 (m, 1H). The spectrum indicates the presence of ca. 0.3 equiv of cocrystallized hexane. $^{31}P\{^1H\}$ NMR (162 MHz, CD_2Cl_2): δ 119.5 (dd, J_{RhP} = 286 Hz, $J_{PP'}$ = 45 Hz), 179.0 (dd, $J_{RhP'}$ = 283 Hz, $J_{PP'}$ = 45 Hz).

Method B. A solution of **2** (261 mg, 0.514 mmol) in dioxane (5 mL) was added dropwise over 5 min to a vigorously stirred light yellow-orange solution of $[RhCl(C_2H_4)_2]_2$ (50.0 mg, 0.119 mmol) in dioxane (4 mL), affording a clear orange solution. The solution was stirred for 2 h and then dried in HV to give a bright orange crystalline solid. The solid was slurried in pentane (10 mL) for 1 h, decanted, and washed with additional pentane (2 × 5 mL). Drying in vacuo yielded 277 mg (94%) of a finely divided orange powder. Spectroscopic data corresponded to those from Method A. Single crystals suitable for X-ray diffraction analysis grew over 7 days from an undisturbed mixture of **8** (110 mg) in CH_3CN (5 mL).

[RhCl((*R*,*R*)-5)$_2$] (9). Benzene (1.6 g) was added to thoroughly mixed $[RhCl(COE)_2]_2$ (101.0 mg, 0.1408 mmol) and (*R*,*R*)-**5** (216.3 mg, 0.5642 mmol), and the resulting deep red solution was stirred overnight. The solution was evaporated to a red solid that was washed with pentane (2 × 6 mL) and then dried in HV to afford an orange powder (225 mg, 88%). Anal. Found: C, 56.51; H, 4.91; N, 3.01. Calcd for $C_{42}H_{44}ClN_2O_8P_2Rh \cdot {}^2/_5C_5H_{12}$: C, 56.58; H, 5.27; N, 3.00. ^{1}H NMR (400 MHz, $CDCl_3$): δ 1.30 (s, 6H), 1.46 (s, 3H), 1.55 (s, 3H), 3.45−4.05 (m, 5H), 4.05−4.40 (m, 6H), 4.85−5.00 (m, 1H), 6.11 (s br, 2H), 6.62 (ABX, J = 35 Hz, 12 Hz, 2H), 6.95−7.50 (m, 14H), 7.55−7.75 (m, 2H). The spectrum indicates the presence of ca. 0.4 equiv of cocrystallized pentane. $^{31}P\{^1H\}$ NMR (162 MHz, toluene-d_8): δ 121.9 (dd, J_{RhP} = 268 Hz, $J_{PP'}$ = 53.4 Hz), 152.9 (dd, $J_{RhP'}$ = 278 Hz, $J_{PP'}$ = 53.4 Hz). ^{13}C NMR (101 MHz, $CDCl_3$): δ 14.1, 22.4, 26.7, 26.8, 27.0, 27.1, 64.6, 65.7, 65.9, 66.3, 68.0, 68.1, 78.3, 78.8, 79.5, 89.1, 89.9, 111.0, 112.2, 126.6, 127.4, 127.5, 127.7, 128.1, 128.6, 128.8, 129.0, 130.0, 130.4, 130.8, 131.0, 136.1, 136.3, 139.6, 140.5−142.0 (m).

[RhCl((*S*,*S*)-6)$_2$] (10). A solution of (*S*,*S*)-**6** (694.4 mg, 2.065 mmol) in benzene (4 g) was added dropwise over 10 min to a vigorously stirred orange slurry of $[RhCl(COD)]_2$ (254.5 mg, 0.5161 mmol) in benzene (2 g) to afford first a clear deep orange solution. Within minutes under stirring copious amounts of a bright orange solid started to precipitate and this mixture was stirred overnight. The solid was separated by filtration (glass fiber GF/B), dried in vacuo, slurried and washed with pentane (12 mL), and dried under HV. Yield: 762 mg (91%), orange powder. Anal. Found: C, 54.70; H, 4.35; N, 6.84. Calcd for $N_4O_4P_2RhClC_{38}H_{34} \cdot H_2O$: C, 55.05; H, 4.38; N, 6.76. ^{1}H NMR (400 MHz, $CDCl_3$): δ 1.20−1.35 (m, 1H), 1.40−1.55 (m, 2H), 1.65−2.20 (m, 7H), 2.75−2.85 (m, 1H), 2.95−3.10 (m, 1H), 4.05−4.15 (m, 1H), 4.35−4.50 (m, 1H), 6.40−6.50 (m, 1H), 6.60−6.80 (m, 2H), 7.03 (d, 1H), 7.10−7.15 (m, 6H), 7.15−7.40 (m, 6H), 7.45−7.60 (m, 3H), 8.40 (d, 1H). $^{31}P\{^1H\}$ NMR (162 MHz, C_6D_6): δ 135.2 (J_{RhP} = 258 Hz, $J_{PP'}$ = 60 Hz), 175.7 (J_{RhP} = 250 Hz, $J_{PP'}$ = 59.5 Hz). ^{13}C NMR (101 MHz, $CDCl_3$): δ 26.0, 26.5, 28.7, 30.2, 47.7, 47.8, 51.8, 52.0, 60.6, 61.5, 93.2, 93.5, 100.7, 100.8, 127.1, 127.4, 127.8, 127.9, 128.0, 128.4, 129.0, 129.2, 129.4, 129.5, 129.6, 130.1, 130.4, 130.7, 130.8, 131.2, 131.6, 135.8, 137.7, 138.5, 139.7, 140.7, 140.8, 141.3, 141.5, 142.7, 172.1, 172.6. Single crystals suitable for X-ray diffraction were obtained by not disturbing the clear reaction solution that formed immediately after addition of the ligand was complete.

[Rh((*S*)-2)$_2$]BF$_4$ (11). A solution of $AgBF_4$ (195.8 mg, 1.006 mmol) in THF (10 g) was added dropwise over 15 min to a vigorously stirred orange slurry of **8** (1217.2 mg, 1.0032 mmol) in THF (15 g), resulting in a deep red mixture which was stirred for 4 h. The volatiles were then evaporated in vacuo, and the product was extracted with CH_2Cl_2 (13 g) by GF/B glass fiber filtration. The clear blood red solution was evaporated to dryness and the residue slurried in Et_2O (8 g) overnight. The solid was separated by filtration and dried in HV to yield 392 mg (95%) of a red powder. Anal. Found: C, 67.69; H, 3.64; N, 2.36. Calcd for $RhBF_4C_{68}H_{44}N_2O_4P_2$: C, 67.79; H, 3.68; N, 2.33. ^{1}H NMR (400 MHz, CD_2Cl_2): δ 5.51 (d, 9 Hz, 2H), 6.38 (d, 8 Hz, 2H), 6.52 (d, 10 Hz, 2H), 6.62 (d, 9 Hz, 2H), 6.65−6.75 (m, 2H), 6.82 (d, 8 Hz, 2H), 6.85−6.95 (m, 2H), 6.95−7.05 (m, 2H), 7.15 (d, 9 Hz, 2H), 7.15−7.25 (m, 2H), 7.25−7.40 (m, 8H), 7.40−7.45 (m, 2H), 7.65−7.95 (m, 12H), 7.95−8.05 (m, 2H). $^{31}P\{^1H\}$ NMR (162 MHz, CD_2Cl_2): δ 165.7 (d, J_{RhP} = 280 Hz). Quantitative ^{13}C NMR (101 MHz, $CDCl_3$): δ 100.5 (br, 2C), 107.8 (br, 2C), 119.2 (2C), 120.3 (m, 4C), 122.7 (2C), 125.4 (2C), 125.5−126.8 (m, 10C), 128.1 (2C), 128.5 (2C), 128.7 (2C), 129.2−130.2 (m, 12C), 130.9 (m, 4C), 131.7 (m, 8C), 132.8 (2C), 136.6 (2C), 139.4 (m, 2C), 140.0 (m, 4C), 145.3 (2C), 147.2 (m, 2C).

[Rh((*S*,*S*)-6)$_2$]BF$_4$ (12). A solution of $AgBF_4$ (50.2 mg, 0.258 mmol) in toluene (3 g) was added dropwise over 10 min to a vigorously stirred slurry of **10** (208.8 mg, 0.2575 mmol) in toluene (8 g), immediately forming a large amount of a brick red flocculating solid and a colorless supernatant solution. The solid was separated by filtration (GF/B) and dried in vacuo, after which CH_2Cl_2 (4 g) was added to afford a blood red solution and a fine white precipitate. Separation by filtration (GF/B), evaporation of the red solution, and washing of the resultant red solid by slurrying in hexane (3 g) for 4 h yielded 208 mg (90%) of a dark red solid. Anal. Found: C, 48.54; H, 3.94; N, 5.60. Calcd for $RhBF_4C_{38}H_{34}N_4P_2O_4 \cdot CH_2Cl_2 \cdot H_2O$: C, 48.53; H, 3.97; N, 5.80. ^{1}H NMR (400 MHz, $CDCl_3$): δ 1.30−1.55 (m, 4H), 1.75−1.95 (m, 2H), 1.95−2.10 (m, 2H), 2.10−2.25 (m, 2H), 2.60−2.80 (m, 2H), 3.90−4.10 (m, 2H), 6.75−6.95 (m, 4H), 7.00−7.35 (m, 6H), 7.35−7.55 (m, 4H), 7.55−7.70 (m, 2H), 7.70−7.85 (m, 2H), 7.85- 8.00 (m, 2H). The spectrum indicates the presence of CH_2Cl_2. $^{31}P\{^1H\}$ NMR (162 MHz, $CDCl_3$): δ 161.5 (d, J_{RhP} = 256 Hz). ^{13}C NMR (101 MHz, $CDCl_3$): δ 25.8, 28.8, 48.9, 61.1, 104.3, 111.3, 128.7, 129.2, 129.8, 129.9, 130.7, 130.8, 131.3, 131.9, 137.7, 138.2, 138.7, 140.7.

[Rh((*S*,*S*)-2)$_2$(quinoline)]BF$_4$ (13). A solution of quinoline (79 mg, 0.61 mmol) in CH_2Cl_2 (5 g) was added dropwise at ca. 270 K

(33) Van der Ent, A.; Onderlinden, A. L.; Schunn, R. A. *Inorg. Synth.* **1990**, *28*, 90.

over 10 min to a vigorously stirred blood red solution of [Rh((*S,S*)-**2**)$_2$]$BF_4 \cdot {}^2/_5Et_2O$ (**11**, 289.0 mg, 0.2341 mmol) in CH_2Cl_2 (5 g) to afford an orange solution that was stirred for 2 h and then evaporated to dryness. This left a microcrystalline, free-flowing orange-red powder that was washed with Et_2O (12 mL). Separation by filtration and drying in vacuo afforded 290 mg (92%) of an orange powder. Anal. Found: C, 68.99; H, 3.95; N, 3.06. Calcd for $RhBF_4C_{77}H_{51}P_2O_4N_3$: C, 69.33; H, 3.85; N, 3.15. ^{1}H NMR (400 MHz, $CDCl_3$): δ 4.30−4.40 (m, 1H), 4.55−4.65 (m, 2H), 4.65−4.75 (m, 1H), 5.25−5.30 (m, 1H), 5.55−5.65 (m, 1H), 5.95−6.10 (m, 2H), 6.35−6.45 (m, 1H), 6.45−6.65 (m, 3H), 6.65−6.75 (m, 2H), 6.80−6.90 (m, 3H), 6.95−7.15 (m, 8H), 7.20−7.90 (m, 16H), 8.05−8.25 (m, 5H), 8.30−8.40 (m, 2H), 8.50−8.60 (m, 1H), 8.85−8.95 (m, 1H), 9.35−9.45 (m, 1H). ^{31}P-{^{1}H} NMR (162 MHz, CD_2Cl_2): δ 115.7 (dd, J_{RhP} = 299 Hz, $J_{PP'}$ = 59 Hz), 182.1 (dd, $J_{RhP'}$ = 246 Hz, $J_{PP'}$ = 59 Hz). ^{13}C NMR (101 MHz, $CDCl_3$): δ 88.9 (m), 96.9, 118.7, 120.6, 121.2, 122.0−123.0 (m), 125.0−132.5 (m), 136.3, 137.7, 138.1 (m), 139.0 (m), 139.3, 140.5−141.0 (m), 147.0−148.5 (m), 150.7, 156.0.

[Rh((*S,S*)-2)$_2$(imidazole)$_2$]$BF_4 \cdot {}^3/_5Et_2O$ (14). A solution of imidazole (35.4 mg, 0.520 mmol) in CH_2Cl_2 (5 g) was added dropwise at ca. 270 K over 10 min to a vigorously stirred, blood red solution of [Rh((*S,S*)-**2**)$_2$]$BF_4 \cdot {}^2/_5Et_2O$ (**12**; 301.5 mg, 0.2478 mmol) in CH_2Cl_2 (5 g) to afford a bright yellow solution that was stirred for 2 h and then evaporated to dryness. This left a microcrystalline, free-flowing lemon yellow solid that was washed with Et_2O (2 × 7 mL). Separation by filtration and drying in vacuo afforded 325 mg (95%) of a fine yellow powder. Anal. Found: C, 65.24; H, 4.28; N, 6.00. Calcd for $RhBF_4C_{74}H_{52}P_2O_4N_6 \cdot {}^3/_5Et_2O \cdot H_2O$: C, 65.39; H, 4.31; N, 5.99. ^{1}H NMR (400 MHz, CD_2Cl_2): δ 5.18 (br, 2H), 5.43 (br, 2H), 5.60 (br, 2H), 6.14 (br, 1H), 6.16 (br, 1H), 6.25−6.40 (m, 4H), 6.55−6.70 (m, 4H), 6.70−6.80 (m, 2H), 6.95−7.15 (m, 7H), 7.15−7.30 (m, 6H), 7.30−7.40 (m, 2H), 7.40−7.50 (m, 2H), 7.60−7.85 (m, 13H), 7.90−7.95 (m, 2H), 11.63 (br, 2H). The spectrum indicates the presence of ca. 0.6 equiv of Et_2O. ^{31}P{^{1}H} NMR (162 MHz, $CDCl_3$): δ 147.8 (d, J_{RhP} = 273 Hz). ^{13}C NMR (101 MHz, $CDCl_3$): δ 120.6, 121.5, 122.1, 124.8, 125.0, 125.2, 125.8, 126.0, 126.2, 126.5−131.5 (m), 131.7, 132.2, 132.9, 134.9, 135.9, 138.3 (m), 141.3, 142.2 (m), 147.7, 149.1. The spectrum indicates the presence of Et_2O.

[CuI((*S*)-2)$_2$] (15). Benzene (16 g) was rapidly added to CuI (616.2 mg, 3.235 mmol) and (*S*)-**2** (3322 mg, 6.472 mmol), and the resulting mixture was stirred for 24 h, affording a white precipitate and a yellow supernatant solution. The solid was separated by filtration (GF/B) and dried in vacuo to yield 3.76 g (93%) of a white powder. Anal. Found: C, 68.50; H, 3.63; N, 2.25. Calcd for $N_2O_4P_2CuC_{68}H_{44}I \cdot {}^1/_2C_6H_6$: C, 68.52; H, 3.81; N, 2.25. ^{1}H NMR (400 MHz, C_6D_6): δ 5.74 (br, 1H), 6.17 (m, 2H), 6.30 (br, 1H), 6.42 (m, 2H), 6.55−6.75 (m, 8H), 6.90−7.00 (m, 4H), 7.00−7.20 (m, 10H), 7.30−7.45 (m, 8H), 7.60 (m, 2H), 7.69 (m, 2H), 7.80 (m, 2H), 8.43 (br, 2H). The spectrum indicated the presence of ca. 0.5 equiv of cocrystallized benzene. ^{31}P{^{1}H} NMR (162 MHz, C_6D_6): δ 120 (br). Single crystals suitable for an X-ray diffraction analysis were obtained by dissolving the complex (78 mg) in boiling benzene (1.2 g) and slowly cooling the solution to room temperature.

[CuI((*S,S*)-4)$_2$] (16). Benzene (20 mL) was rapidly added to a mixture of CuI (382.8 mg, 2.010 mmol) and (*S,S*)-**4** (1.908 g, 4.021 mmol) with vigorous stirring, and the resulting clear pale yellow solution was stirred for 8 h. Evaporation of the volatiles afforded an off-white solid which was pure enough for most applications. The product was recrystallized by dissolving it in hot toluene (20 mL), followed by filtration over glass fiber (GF/B) and cooling to 250 K for 2 days. The resulting white crystals were separated from the mother liquor by decanting and were dried in vacuo (1.16 g, 51%). This batch afforded single crystals suitable for an X-ray diffraction analysis. The mother liquor was concentrated to ca. 10 mL, Et_2O (15 mL) was added, and the mixture kept at 250 K for 2 days to afford another crop of white microcrystals (0.75 g, 33%). Anal. Found: C, 64.87; H, 4.53; N, 4.86. Calcd for $CuIN_4O_2P_2C_{62}H_{54} \cdot {}^1/_2H_2O$: C, 64.84; H, 4.83; N, 4.88. ^{1}H NMR (400 MHz, C_6D_6): δ 0.90−1.05 (m, 2H), 1.20−1.45 (m, 6H), 2.85−2.95 (m, 2H), 3.45−3.55 (m, 2H), 3.55−3.75 (br, 2H), 6.55−6.70 (m, 6H), 6.80−7.40 (m, 28H), 7.40−7.55 (m, 6H). ^{31}P{^{1}H} NMR (162 MHz): δ 116 (br, C_6D_6); 114 (br, CD_2Cl_2). Quantitative ^{13}C NMR (101 MHz, CD_2Cl_2): δ 27.1 (s, 2C), 29.1 (s, 2C), 46.0 (s, 2C), 68.7 (s, 2C), 94.3 (s, 2C), 126.0−129.0 (m, 34C), 129.4 (s, 2C), 130.0 (s, 4C), 132.3 (s, 2C), 137.0 (s, 2C), 137.8 (s, 2C), 140.4 (s, 2C), 142.2 (s, 2C), 144.0 (s, 2C), 145.6 (s, 2C).

[CuI((*R,R*)-5)$_2$] (17). Benzene (3 g) was added to CuI (93.5 mg, 0.491 mmol) and (*R,R*)-**5** (376 mg, 0.982 mmol), and the resulting mixture was stirred, forming a clear pale yellow solution within 5 min. The solution was stirred overnight, and then the volatiles were evaporated, affording a white solid which was slurried in pentane (8 mL) for 12 h and then separated by filtration. HV drying afforded 378 mg (80%) of a fine white solid. Anal. Found: C, 51.80; H, 4.50; N, 2.84. Calcd for $CuIN_2O_8P_2C_{42}H_{44} \cdot H_2O$: C, 51.73; H, 4.75; N, 2.87. ^{1}H NMR (400 MHz, C_6D_6): δ 1.21 (s, 6H), 1.33 (s, 6H), 3.50−3.65 (m, 2H), 3.75−3.85 (m, 2H), 3.90−4.10 (m, 6H), 6.60−6.70 (m, 4H), 6.85−7.05 (m, 8H), 7.05−7.20 (m, 4H), 7.60−7.70 (m, 4H). ^{31}P{^{1}H} NMR (162 MHz, C_6D_6): δ 116 (s, br). ^{13}C NMR (101 MHz, C_6D_6): δ 26.8 (d, 28 Hz), 65.0 (d, 11 Hz), 78.9, 79.6, 110.9, 126.6 (d, 5 Hz), 128.8, 129.1, 129.3, 129.4, 131.0, 131.6, 136.3 (d, 7 Hz), 142.1, 142.6 (d, 11 Hz).

Cu((*S*)-2)$_2$(BF$_4$) (18). A solution of $AgBF_4$ (156.2 mg, 0.8023 mmol) in THF (10 g) was added dropwise over 10 min to a vigorously stirred clear, colorless solution of **15** (1011 mg, 0.7985 mmol) in THF (12 g) to afford a greenish white precipitate with a colorless supernatant. The mixture was stirred for 24 h, the precipitate separated by centrifugation (4000 rpm, 60 min), and the clear supernatant solution was evaporated to dryness and the white solid dried in HV (915 mg, 98%). Anal. Found: C, 67.28; H, 3.78; N, 2.15. Calcd for $C_{68}H_{44}CuP_2N_2O_4BF_4 \cdot 2.5H_2O$: C, 67.48; H, 4.08; N, 2.31. ^{1}H NMR (400 MHz, CD_2Cl_2): δ 5.10−5.25 (m br, 2H), 6.20−6.30 (m, 2H), 6.35−6.55 (m, 4H), 6.60−6.80 (m, 4H), 6.85−7.05 (m, 8H), 7.05−7.45 (m, 12H), 7.50−7.60 (m, 4H), 7.75−7.85 (m, 2H), 7.90−8.00 (m, 2H), 8.05−8.15 (m, 2H), 8.20−8.30 (m, 2H). ^{31}P{^{1}H} NMR (162 MHz, CD_2Cl_2): δ 114 (s, br). ^{13}C NMR (101 MHz, CD_2Cl_2): δ 120.4, 120.7, 122.4, 122.8, 125.3, 125.6, 126.2, 126.4 (m, br), 126.5, 126.8, 127.0 (br), 128.2, 128.5, 128.6, 129.0, 129.2, 129.3, 129.6, 129.7, 130.8, 131.2, 131.4, 131.8, 132.3, 132.8, 135.0, 136.1, 139.7, 140.4 (m) 147.2, 147.6 (m). Large single crystals grew from a filtered (cotton plug plus Celite) warm solution of the compound (120 mg) in toluene (4.5 g).

Cu(BF$_4$)((*R,R*)-4)$_2$·THF (19). A solution of $AgBF_4$ (87.1 mg, 0.447 mmol) in THF (6 g) was added dropwise over 10 min to a vigorously stirred clear, colorless solution of **16** (508.5 mg, 0.4462 mmol) in THF (6 g) to afford a greenish white precipitate with a colorless supernatant. The mixture was stirred for 8 h. The solid was separated by filtration, dried in vacuo, and then extracted with CH_2Cl_2 (16 g) by filtration (GF/B glass fiber). The clear mother liquor was evaporated to an off-white solid that was slurried in THF (5 mL) for 30 min, separated by filtration, and finally dried in HV to afford 382 mg (73%) of a snow white powder. This material is usually 95% isomerically pure (the impurity is characterized by a pair of doublets in the ^{31}P{^{1}H} NMR spectrum; see below). The impurity was removed by successive washings in benzene. Anal. Found: C, 65.72; H, 5.03, N, 4.68. Calcd for $CuBF_4N_4O_2P_2C_{62}H_{54} \cdot C_4H_8O \cdot {}^1/_2CH_2Cl_2$: C, 65.79; H, 5.23; N, 4.62. ^{31}P{^{1}H} NMR (162 MHz, C_6D_6): δ 106 (s, br), isomeric impurity (5−8%): 116 (d, $J_{PP'}$ = 53 Hz), 121 (d, $J_{PP'}$ = 53 Hz). ^{1}H NMR (400 MHz, C_6D_6): δ 1.10−1.25 (m, 2H), 1.50−1.60 (m, 2H), 1.60−1.80 (m, 6H), 1.85−1.95 (m, 2H), 2.85−3.00 (m, 4H), 3.00−3.10 (m, 2H), 3.35−3.50 (m, 4H), 6.45−6.50 (m, 2H), 6.65−6.75 (m, 2H), 6.85−6.95 (m, 2H), 6.95−7.05 (m, 2H), 7.05−7.45

Table 5. Crystal Data and Data Collection Parameters of Complexes 8, 10, 12, 15, and 16

	8	10	12	15	16
formula	$C_{72}H_{50}ClN_4O_4P_2Rh$	$C_{38}H_{34}ClN_4O_4P_2Rh$	$C_{39}H_{36}BCl_2F_4N_4O_4P_2Rh$	$C_{80}H_{58}CuIN_2O_6P_2$	$C_{62}H_{54}CuIN_4O_2P_2$
M_r	1235.46	810.99	947.28	1395.66	1139.47
cryst syst	monoclinic	orthorhombic	monoclinic	orthorhombic	monoclinic
space group	$P2_1$	$P2_12_12_1$	$P2_1$	$P2_12_12$	$P2_1$
a (Å)	13.369(4)	10.1359(7)	12.926(4)	13.686(3)	12.040(5)
b (Å)	18.019(4)	14.4717(10)	12.530(3)	24.927(5)	18.120(6)
c (Å)	13.741(4)	24.2819(18)	13.177(3)	10.4443(19)	13.188(5)
β (deg)	117.416(5)		92.392(7)		112.916(9)
V (Å^3)	2938.3(14)	3561.8(4)	2132.2(10)	3.563.1(11)	2.649.9(16)
Z	2	2	2	2	2
μ (mm^{-1})	0.45	0.69	0.66	0.84	1.10
D_c (g cm^{-3})	1.396	1.512	1.475	1.301	1.428
no. of rflns collected	33 295	40 663	24 255	40 609	27 074
no. of indep rflns, R_{int}	11 092, 0.052	7167, 0.059	8056, 0.074	7526, 0.058	9256, 0.042
GOF	1.09	1.14	1.06	1.08	1.08
R1, wR2 ($I > 2\sigma(I)$)	0.051, 0.117	0.044, 0.100	0.067, 0.191	0.068, 0.19	0.044, 0.132
max, min features in final diff map (e Å^{-3})	0.63, −0.59	0.97, −0.820	0.80, −0.65	0.51, −0.47	0.72, −1.14

(m, 24H), 7.45−7.60 (m, 8H). The spectrum indicates the presence of ca. 0.5 equiv of CH_2Cl_2 of cocrystallization. ^{13}C NMR (101 MHz, CD_2Cl_2): δ 25.6 (THF), 27.3, 28.6, 44.9 (m), 69.3 (THF), 70.8, 95.6, 126.7, 127.1, 127.3, 127.8, 127.9, 128.0, 128.2, 128.26, 128,31, 129.0, 129.8, 129.9, 130.3, 130.6, 131.3, 136.2, 136.9, 139.4, 140.9, 143.7.

Crystal Structure Determinations. Intensity data were recorded at room temperature on a Rigaku AFC-7S diffractometer using monochromated Mo Kα radiation (λ = 0.710 73 Å). Experimental details on unit cell and intensity measurements can be found in the CIF files deposited with the Cambridge Crystallographic Data Centre under deposition numbers CCDC 770993−770997 corresponding to complexes **8**, **10**, **12**, **15**, and **16**, respectively. Crystal data, intensity data collection parameters and final refinement results are summarized in Table 5. An empirical absorption correction (multiscan) was applied to all the data using the CrystalClear crystallographic software package.[34] The structures were solved by direct methods and refined by full-matrix least squares on F^2. The H atoms on C were placed in calculated positions using a riding atom model with fixed C−H distances (0.93 Å for C(sp^2), 0.96 Å for C(sp^3, CH_3), and 0.97 Å for C(sp^3, CH_2)). All the H atoms were refined with isotropic displacement parameters set to 1.2U_{eq} for C(sp^2) and 1.5U_{eq} for C(sp^3) of the attached atom. In structure **8**, two acetonitrile molecules were found, one of which was found disordered over two sets of positions. The occupational parameters were refined to 46:54. In structure **12** either a BF_4^- anion or a dichloromethane molecule was found disordered. For each molecule the disorder was modeled over two orientations with restraints in the B−F, C−Cl, and Cl···Cl distances and with complementary occupancies of 73:27 and 48:52 for the anion and dichloromethane, respectively. In structure **15** the dibenz[*b*,*f*]azepine unit was found disordered over two sets of positions, which were included by constraining the aromatic rings to a regular hexagon. The occupational parameters were refined to 59:41. Also, either benzene or water molecules were found disordered. For each molecule the disorder was modeled over two orientations. The benzene ring was refined by constrainment to a regular hexagon, obtaining complementary occupancies of 50:50. The water molecule was refined with isotropic displacement parameters only. All the refinement calculations were made using SHELXTL-NT.[35]

General Procedure for the 1,4-Addition of Boronic Acids to Enones. Inside the glovebox a 20 mL vial was charged with Rh precatalyst (0.0075 mmol), boronic acid (0.6 mmol), and a stirring bar. Dioxane was added (1 mL), and the vial was sealed with a PTFE cap and removed from the glovebox. Degassed enone (0.5 mmol) and degassed KOH solution (2.5 M in H_2O, 0.1 mL, 0.25 mmol) were added via syringe. The mixture was stirred at 40 or 60 °C for 1 h. After this time, it was diluted with Et_2O (10 mL) and washed with water (2 × 10 mL). The organic phase was dried over $MgSO_4$ and the solvent evaporated. The product was purified by flash chromatography (silica gel G60, 9:1 hexane/Et_2O eluent) and analyzed by NMR and HPLC. Compounds **22Aa**−**22Ah**, **22Ba**, and **22Ea** have been previously reported.[1]

(*R*)-4-Phenylpentan-2-one (22Ca):[36] eluted with hexane/ether (50/1), obtained as a yellow oil. HPLC conditions: Chiralcel OJ-H column (hexane/*i*-PrOH 98/2, 0.7 mL/min); t_R 23.0 min (minor), 25.1 min (major). ^1H NMR (400 MHz, $CDCl_3$): δ 1.25 (d, J = 6.9 Hz, 3H), 2.04 (s, 3H), 2.61−2.77 (m, 2H), 3.24−3.33 (m, 1H), 7.17−7.20 (m, 3H), 7.26−7.29 (m, 2H). ^{13}C NMR (100 MHz, $CDCl_3$): δ 22.31 (s), 30.88 (s), 35.77 (s), 52.32 (s), 126.62 (s), 127.07 (s), 128.86 (s), 146.49 (s), 208.12 (s).

(*R*)-4-Phenylheptan-2-one (22Da):[37] eluted with hexane/ether (50/1), obtained as a colorless oil. HPLC conditions: chiralcel OJ-H column (hexane/*i*-PrOH 99.5/0.5, 0.5 mL/min); t_R 24.2 min (minor), 26.1 min (major). ^1H NMR (400 MHz, $CDCl_3$): δ 0.90 (t, J = 7.3 Hz, 3H), 1.26−1.29 (m, 2H), 1.56−1.70 (m, 2H), 2.07 (s, 3H), 2.71−2.82 (dd, J = 7.2 Hz and J = 3.3 Hz, 2H), 3.15−3.22 (m, 1H), 7.22−7.26 (m, 3H), 7.32−7.36 (m, 2H). ^{13}C NMR (100 MHz, $CDCl_3$): δ 14.26 (s), 20.82 (s), 30.95 (s), 39.00 (s), 41.38 (s), 51.24 (s), 126.61 (s), 127.78 (s), 128.75 (s), 144.88 (s), 208.31 (s).

(*R*)-4-Phenylnonan-2-one (22Fa):[38] eluted with hexane/ether (50/1), obtained as a colorless oil. HPLC conditions: chiralcel OJ-H column (hexane/*i*-PrOH 98/2, 0.5 mL/min); t_R 12.5 min (major), 14.2 min (minor). ^1H NMR (400 MHz, $CDCl_3$): δ 0.80 (t, J = 6.9 Hz, 3H), 1.09−1.24 (m, 6H), 1.53−1.64 (m, 2H), 1.99 (s, 3H), 2.69 (dd, J = 7.2 and J = 2.2), 3.07−3.11 (m, 1H), 7.14−7.18 (m, 3H), 7.24−7.28 (m, 2H). ^{13}C NMR (100 Hz, $CDCl_3$): δ 14.27 (s), 22.75 (s), 27.30 (s), 30.90 (s), 31.99 (s), 36.70 (s), 41.59 (s), 51.23 (s), 126.56 (s), 126.56 (s), 127.73 (s), 128.71 (s), 144.90 (s), 208.27 (s).

(*R*)-4-Phenyl-5-methylhexan-2-one (22Ga):[38] eluted with hexane/ether (50:1), obtained as a colorless oil. HPLC conditions: chiralcel OJ-H column (hexane/*i*-PrOH, 99:1, 1 mL/min); t_R 9.7

(34) *CRYSTALCLEAR, Software Users Guide, Version 1.3.6*; Rigaku/MSC: The Woodlands, TX, 2000.

(35) *SHELXTL-NT, Version 5.1*; Bruker AXS Inc., Madison, WI, 1998.

(36) Shintani, R.; Kimura, T.; Hayashi, T. *Chem. Commun.* **2005**, 3213.

(37) Feng, C.; Wang, Z.; Shao., C.; Xu, M.; Lin, G. *Org. Lett.* **2008**, *10*, 4101.

(38) Okamoto, K.; Hayashi, T.; Rawal, V. H. *Org. Lett.* **2008**, *10*, 4387.

min (major), t_R11.6 min (minor). ^{1}H NMR (400 MHz, $CDCl_3$): δ 0.75 (d, J = 6.7 Hz, 3H), 0.93 (d, J = 6.6 Hz, 3H), 1.79−1.87 (m, 1H), 1.97 (s, 3H), 2.78−2.80 (m, 2H), 2.89−2.94 (m, 1H), 7.12−7.20 (m, 3H), 7.24−7.28 (m, 2H). ^{13}C NMR (100 MHz, $CHCl_3$) δ: 20.60 (s), 20.99 (s), 30.86 (s), 33.58 (s), 47.95 (s), 48.38 (s), 126.55 (s), 128.45 (s), 128.54 (s), 143.51 (s), 208.5 (s).

General Procedure for the 1,4-Addition of $AlEt_3$ to Enones. Inside the glovebox a 20 mL vial was charged with Cu precatalyst (0.01 mmol for **16**−**20**) as a solution in 1,2-dichloroethane (2 mL) and a stirring bar. The vial was sealed with a PTFE cap and taken outside the glovebox. Degassed enone (0.5 mmol) and degassed dodecane (0.5 mmol, as internal standard) were then added via syringe. The vial was cooled to −25 °C and $AlEt_3$ was added dropwise via syringe, so as not to increase the temperature. The reaction was analyzed by GC (chiral column Lipodex E, 25 m × 0.25 mm) to obtain values for conversion and enantiomeric excess. The product was isolated and confirmed by comparison with literature values.[18b]

Acknowledgment. We thank the FONACIT (Projects S1-2001000851 and LAB-97000821) for financial support, Ms. Noelani Cigüela for technical assistance (NMR laboratory, USB), and Prof. Giuseppe Agrifoglio for helpful discussions.

Supporting Information Available: CIF files giving crystal structure data for complexes **8**, **10**, **12**, **15**, and **16**. This material is available free of charge via the Internet at http://pubs.acs.org.